Integrated Analytic and Linearized Inverse Kinematics for Precise Full Body Interactions

View metadata, citation and similar papers at core.ac.uk

brought to you by CORE

provided by Infoscience - École polytechnique fédérale de Lausanne

Ronan Boulic and Daniel Raunhardt

VRLAB, Ecole Polytechnique Fédérale de Lausanne, EPFL
1015 Lausanne, Switzerland
{Ronan.Boulic,Daniel.Raunhardt}@epfl.ch
http://vrlab.epfl.ch

Abstract. Despite the large success of games grounded on movement-based interactions the current state of full body motion capture technologies still prevents the exploitation of precise interactions with complex environments. This paper focuses on ensuring a precise spatial correspondence between the user and the avatar. We build upon our past effort in human postural control with a Prioritized Inverse Kinematics framework. One of its key advantage is to ease the dynamic combination of postural and collision avoidance constraints. However its reliance on a linearized approximation of the problem makes it vulnerable to the well-known full extension singularity of the limbs. In such context the tracking performance is reduced and/or less believable intermediate postural solutions are produced. We address this issue by introducing a new type of analytic constraint that smoothly integrates within the prioritized Inverse Kinematics framework. The paper first recalls the background of full body 3D interactions and the advantages and drawbacks of the linearized IK solution. Then the Flexion-EXTension constraint (FLEXT in short) is introduced for the partial position control of limb-like articulated structures. Comparative results illustrate the interest of this new type of integrated analytical and linearized IK control.

1 Introduction

For a movement-based game to be successful a good match is needed between the mapping of sensed user gestures in the game space and a sufficiently challenging goal to achieve within that space. There is no need of highly precise full-body mapping in the game space as long as the 'flow' and 'engagement' of the user are maintained. These two concepts are central to the analysis and design of movement-based interactions as extensively reviewed in [NvDR08]. They help to understand that the player can accommodate large discrepancies between their egocentric space and the virtual space of the game. For example, Loke et al. analyze multiple framework for interaction design that aim to identify the best exploitation of bodily interactions with a given technology ; the paper is illustrated with two Sony Eyetoy games [LLRE07].

Conversely, a highly precise spatial correspondence of the user and the avatar is a basic requirements of virtual prototyping applications for which important design decisions have to be made based on 3D immersive interactions. However, even now few motion capture hardware and software can provide a robust and precise real-time

A. Egges, R. Geraerts, and M. Overmars (Eds.): MIG 2009, LNCS 5884, pp. 231–242, 2009.
© Springer-Verlag Berlin Heidelberg 2009

participant registration with virtual objects and obstacles. The problem is made even more complex whenever the participant wishes to feel immersed as a virtual counterpart with a differing body size as analyzed in [BMT09]. We believe that methods and algorithms tackling such precision issues will find their way in the game sector in the near future.

In this paper we focus on ensuring a precise spatial correspondence between the user equipped with a relevant posture sensing equipment and the avatar. We first review the state of the art on motion capture and Inverse Kinematics (IK) approaches. Our contribution builds upon our past effort in human postural control with a Prioritized Inverse Kinematics framework [BB04]. Such a framework eases the dynamic combination of constraints, e.g. to avoid collisions while performing a reach task [PMMRTB09]. However its reliance on a linearized approximation of the problem makes it vulnerable to the well-known full extension singularity of the limbs illustrated in Figure 1. In such context the convergence performance is degraded and/or less believable intermediate postural solutions are produced.

We address this issue by introducing a new type of constraint that smoothly integrates within the prioritized Inverse Kinematics framework. The proposed Flexion-EXTension (FLEXT) effector takes advantage of the knowledge of the desired 1D displacement along the direction linking the limb root to the controlled effector (chain tip square on Figure 1). Comparative results illustrate the interest of this new type of IK effector.

2 Background in Full Body 3D Interactions

The field of applications relying on full body interactions traces back to the sixties as reviewed by Sturman [S98]. In the early days mechanical exoskeleton were (tediously) adjusted to the performer for live performance in various shows. However such technology is too intrusive to be accepted by engineers or gamers. Nowadays the trend is clearly towards transparent and ubiquitous systems such as marker-free vision-based approaches. For example Michoud et al. report performances compatible with real-time full-body interactions [MGBB07]. Yet the approach is limited to the identification of eleven body joints due to the coarse resolution of the underlying voxel grid ; besides its reliance on a static background for silhouette processing limits its application in more versatile contexts. In the nineties a seducing alternative to vision-based techniques was to exploit magnetic sensors as they are not subject to occlusion [A96]. Molet et al [MBRT99] proposed an analytic IK algorithm exploiting one 3D orientation measurement per body segment and one 3D position measurement for the whole body. It has been exploited in a real-time full-body tennis game demonstrated at the international exhibition Telecom Interactive‘97 in Geneva [M*99]. Its major drawback was however the heavy calibration effort to obtain homogeneous position measurement over the capture area [MBRT99]. A true improvement came with the advent of active optical motion capture systems that could automatically recognize the markers even after some periods of occlusion (e.g. [P]). Although not as precise as some optical systems exploiting high tech cameras with passive markers [V] we tradeoff the extra precision for the real-time marker identification. In the remainder of the section we review various approaches of on the fly postural reconstruction from a set of 3D locations, further denoted as position *effectors*.

Analytic methods have always been the most efficient approaches for reconstructing the body posture from the input of desired locations of body parts. One key reference is the work of Korein [K85] from which successive variants and improvements have been proposed. Tolani et al. describe a position and orientation control of the limbs [TGB00] with a special focus on the control of the *swivel* angle along the direction linking the limb root to the controlled effector (visible as a dotted line in Figure 1a). Kulpa et al. build upon the Cyclic Coordinate Descent approach to combine postural and balance control [KMA05]. Kallmann takes advantage of a database of reach postures [K07]. Unzuetta et al. exploits a reduced set of effector locations (pelvis, head, hands and feet) and compares its performances with numerous other analytic and linearized IK approaches [UPBS08]. Despite their low computational cost analytical solutions often suffer from temporary instability. Indeed most of them rely on simplifying assumptions that are violated from time to time. For example, the limb full extension posture is prone to produce discontinuities of the swivel angle.

Linearized Inverse Kinematics approaches are more versatile as they can combine a large variety of constraints in a redundant context. On the down side they are much slower due to the iterative nature of the convergence towards a posture minimizing the constraint errors [BMW87][PB91][ZB94][BB04][UPBS08]. Nevertheless the regular increase in computing power has made it possible to exploit them for full-body 3D immersive interactions [MBT08]. The next section focuses on the numerical problems due to the human postural singularities.

3 The Limb Singular Postures

The limb singular postures (Figure 1) are especially annoying for linearized IK method. The full extension posture (Figure 1b) is very frequent in standing and reaching poses. We have identified two recurrent problems in such singular posture.

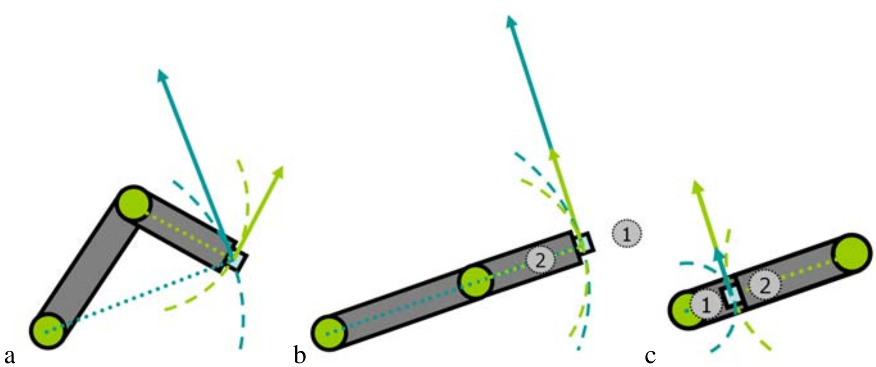

Fig. 1. In the general case the linearized Inverse Kinematic control can move the chain tip effector in any direction (a) but this is no more the case when the two controlled segments are aligned such as in the full extension (b) or the full flexion (c) ; no linearized solution can be found to move the chain tip in the direction of goal 1 or 2 although there exist an analytic solution for goal 2.

The flexing blindness syndrome: when a singularity occurs the limb joints cannot theoretically contribute to move the chain tip effector towards the limb root because the linear influences of the joints are collinear and span only a 1D translation space orthogonal to the desired translation (visible on Fig 1b and c). We call this artefact the flexing blindness syndrome to distinguish it from the second side effect described later. In practice the posture is seldom exactly on the singularity but in the close neighborhood. The use of a damped least square pseudo-inverse ensures that the solution norm remains bounded [M90][BB04] by trading off the convergence speed for stability. This type of context leads to a very slow limb flexing. In the meantime the effector inward movement can be produced by other joints such as the spine or whole body movements. Needless to say that the movement produced by this type of convergence is much less believable than simply flexing the limb.

The rank decrease syndrome: this alternate type of full extension side effect occurs when the posture happens to be considered as theoretically singular by the IK algorithm. In such a context the rank decreases from 2 (Fig 1a) to 1 because the linearized joint influences are collinear and span a 1D space (Fig 1b, c). The consequence of such a rank decrease is the corresponding rank increase of the Null space in the joint variation space. It could be interpreted positively as an opportunity for lower priority constraints to achieve their own goal. In fact the consequence is rather negative as what happens is a posture variation discontinuity introduced by these lower priority constraints. Most of the time the posture variation induced by the low priority constraints leads to a new posture that restores the full rank of the high priority constraint. Therefore this ends the convergence opportunity for the low priority tasks. This convergence pattern can reproduce repeatedly as long as the constraints' goal remain constant. As a consequence, it is highly desirable to prevent such a rank decrease.

The contribution of this paper addresses both kinds of side effects. We now briefly recall the architecture of the linearized Inverse Kinematics with multiple levels of priority prior to describe how to integrate an analytic solution of the limb flexion-extension control into that framework.

4 Basic Concepts of Prioritized Inverse Kinematics

The concept of priority in the linearized IK solution was introduced by Liégeois [L77] and generalized for an arbitrary number of priority levels in [SS91] ; Baerlocher proposed a formulation with a lower computation cost in [BB04]. An extended illustration of the concepts and the algorithm can be found in [BLP06]. In the remainder of this section we simply recall the key aspects and notations related to this approach.

Linearized IK and validity of the solution: a linearized Inverse Kinematics approach replaces the resolution of a general non-linear problem of finding the posture $\boldsymbol{\theta}$ such that

$$\mathbf{x}_{\mathbf{goal}} = \mathbf{f}(\boldsymbol{\theta}) \tag{1}$$

by the resolution of a first order approximation equation

$$\boldsymbol{\Delta}\mathbf{x} = \boldsymbol{J}\,\boldsymbol{\Delta}\mathbf{q} \tag{2}$$

that is valid only in the neighborhood of the current state of the system $(\mathbf{x}_c, \boldsymbol{\theta}_c)$. The Jacobian $\boldsymbol{J}$ is the matrix of the partial derivatives $\boldsymbol{\delta}\mathbf{x}/\boldsymbol{\delta\theta}$ for the current state.

For example, the two vectors displayed for Figure 1a are the partial derivatives of the chain tip position with respect to the limb joints. Inverting equation 2 consists in expressing a desired position variation $\mathbf{\Delta x}$ as a linear combination of those vectors. As one can see from Figure 1 the vectors are in fact only the approximation of the true joints influence shown as arcs. The validity of the approximation degrades as $\mathbf{\Delta x}$ norm increases. Hence equation 2 has to be solved for successive small variations $\mathbf{\Delta x}$ proportional to ($\mathbf{x_{goal}}$ - $\mathbf{x_c}$). As a rule of thumb, the maximum norm of $\mathbf{\Delta x}$ can be expressed as a fraction of the total length of the articulated chain, e.g. 10%. In our case we also scale it by a damping factor between 0 and 1 that prevents instabilities in the close neighborhood of the goal.

It is now easy to see why the limb full extension is singular for flexing the limb (Fig 1b); it is not possible to express a desired $\mathbf{\Delta x}$ in the direction of the limb root as a linear combination of the two collinear vectors stored in the Jacobian $\boldsymbol{J}$. Similarly one can also see the 2 to 1 rank reduction of the space spanned by these two vectors in Figure 1b and 1c.

Redundancy, priority and projection operator: the articulated structure to control is generally redundant with respect to the constraints to achieve, i.e. the dimension **N** of the joint space is much larger than the dimension **M** of the constraint space. The first consequence is the potentially infinite number of posture variations $\mathbf{\Delta\theta}$ that achieve a desired constraint variation $\mathbf{\Delta x}$. The linearized IK architecture retains the one with the smallest (and bounded) norm as provided by a damped pseudo-inverse of the jacobian $\boldsymbol{J}$. For 3D full-body interactions multiple constraints have to be enforced simultaneously ; it is possible to associate a distinct priority level **k** to each of them, or to obtain a compromise solution by integrating them in a single Jacobian. The exploitation of priority levels is preferred to guarantee important properties first, e.g. the avatar feet remains in contact with the floor, etc… In such a case a projection operator

$$\boldsymbol{P_k} = \boldsymbol{I} - \boldsymbol{J_{Ak}}^{+} \boldsymbol{J_{Ak}} \tag{3}$$

is built to avoid low priority solutions to interfere with all higher priority ones gathered in the augmented Jacobian $\boldsymbol{J_{Ak}}$[SS91].

5 The 1D Analytic FLexion-EXTension (FLEXT) Constraint

The proposed Flexion-EXTension (FLEXT) constraint is intimately associated with a limb-like articulated structure corresponding to those present in the human body for the arms and the legs. The considered limb articulated structure is constituted by a ball & socket joint for the root joint and, for the middle joint, the succession of a flexion-extension rotation followed by a twist rotation along the second limb segment. Only the Flexion-extension degrees of freedom of the middle and the root joints are exploited for the proposed constraint (Figure 2a,b). The other degrees of freedom remain free to be exploited by other constraints. The FLEXT constraint concept is illustrated in the ideal case where both limb segments belong to the plane orthogonal to the middle joint flexion-extension axis. A more general case is presented in the appendix A.

The rationale for introducing the new FLEXT constraint is the following :

- The flexibility of the Prioritized IK framework is highly desirable to preserve
- The linearized approximation is satisfactory except in singular contexts
- The singular context occurs frequently in some application such as human motion capture (standing, reaching)
- It is necessary and sufficient to solve ***analytically*** for the posture variation **Δθ** corresponding to a desired *scalar displacement* ***Δx*** along the line linking the effector to the limb root (Figure 2a,b) to prevent the two identified side effects.
- As a consequence, the control of the other effector dimensions (position and orientation) can be left to standard linearized constraints.

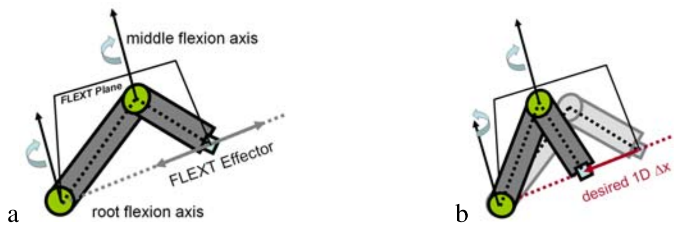

Fig. 2. (a) Definition of the Flexion-Extension 1D controlled translation and the FLEXT plane passing through the root joint whose normal is the flexion axis, (b) solving for a desired scalar displacement ***Δx*** resulting in a coupled variation of the two flexion degrees of freedom ; note that the limb remains within the FLEXT plane

The principle of the proposed approach is to reframe the 1D analytical solution as a linear equality constraint so that it can be transparently integrated in the linearized IK framework.

5.1 Evaluating the Posture Variation Δθ for a Desired Scalar Displacement *Δx*

First let us express the minimal angle variation **(Δα, Δβ)** in the FLEXT plane that achieves the signed scalar displacement ***Δx*** as illustrated in Figure 3 (***Δx*** is negative in this example). The distances **L1, L2, L3** are constant known quantities or can be evaluated from the current limb state. The angles are obtained from the cosine rule:

$$\cos\alpha = (L1^2 - L2^2 + L3^2) \quad /(2\, L1\, L3) \tag{4}$$

$$\cos\alpha' = (L1^2 - L2^2 + (L3 + \Delta x)^2)\, /(2\, L1\, (L3 + \Delta x)) \tag{5}$$

$$\cos\beta = (L1^2 + L2^2 - L3^2) \quad /(2\, L1\, L2) \tag{6}$$

$$\cos\beta' = (L1^2 + L2^2 - (L3 + \Delta x)^2)\; /(2\, L1\, L2) \tag{7}$$

and

$$\Delta\alpha = \alpha' - \alpha \qquad\qquad \Delta\beta = \beta' - \beta \tag{8}$$

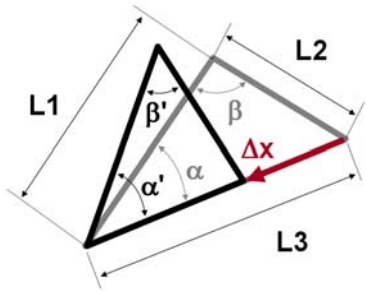

b

Fig. 3. The two triangles highlighting the posture variation of Figure 2b in the FLEXT plane. **L1** is the distance from the root to the middle joint, **L2** is the distance from the middle joint to the effector, **L3** is the initial distance of the effector to the root ; in this example it is decreased by a negative $\boldsymbol{\Delta x}$ displacement.

The limb posture variation $\Delta\theta$ is composed of a component for the root joint and a component for the middle joint ; they can be obtained from the angle variations in the FLEXT plane ($\Delta\alpha$, $\Delta\beta$) as follows:

- By construction of the FLEXT constraint $\Delta\beta$ corresponds to the scalar variation of the middle joint flexion-extension degree of freedom. The middle joint twist variation is null.
- $\Delta\alpha$ has to be converted into a parameter variation of the ball & socket root joint. We exploit the exponential map representation of rotation [G98] but the principle of the conversion remain the same for other choices. It work like this:
  - Express the middle flexion axis in the coordinate system of the first limb segment that takes into account the current root joint transformation. The result is the root flexion axis.
  - Build the rotation matrix $\boldsymbol{R_\alpha}$ of amplitude $\Delta\alpha$ along the root flexion axis.
  - Concatenate $\boldsymbol{R_\alpha}$ to the current joint rotation matrix $\boldsymbol{R}$ to obtain a new rotation matrix $\boldsymbol{R'}$.
  - Convert both $\boldsymbol{R'}$ and $\boldsymbol{R}$ into your chosen rotation parameter ; the difference is the root joint component of the posture variation $\Delta\theta$

5.2 Evaluating the FLEXT Coupling Jacobian $\boldsymbol{J_{FLEXT}}$ and the Task $\boldsymbol{\Delta x_{FLEXT}}$

In order to be transparently integrated within the linearized IK framework, the FLEXT constraint has to provide its Jacobian matrix $\boldsymbol{J_{FLEXT}}$ and its task vector $\boldsymbol{\Delta x_{FLEXT}}$. Given these two entities it can be associated with a priority and integrated in the loop evaluating the prioritized IK solution [BB04]. The FLEXT constraint has one fundamental difference compared to other linearized IK constraints : it exploits the knowledge of the desired scalar displacement $\boldsymbol{\Delta x}$ to build its associated Jacobian line matrix $\boldsymbol{J_{FLEXT}}$ whereas other constraints evaluate separately their Jacobian and their task vector.

Given the desired scalar displacement $\boldsymbol{\Delta x}$ and the corresponding posture variation $\Delta\theta$ (section 5.1) the FLEXT line matrix Jacobian $\boldsymbol{J_{FLEXT}}$ and the task $\boldsymbol{\Delta x_{FLEXT}}$ are given by:

$$\boldsymbol{J_{FLEXT}} = (1 / \|\Delta\theta\|)\, \Delta\theta^T \qquad (9)$$

$$\boldsymbol{\Delta x_{FLEXT}} = \|\Delta\theta\| \qquad (10)$$

$\boldsymbol{J_{FLEXT}}$ being a unit vector its pseudo-inverse is given by:

$$\boldsymbol{J_{FLEXT}}^+ = \boldsymbol{J_{FLEXT}}^T \qquad (11)$$

Hence the product of the pseudo-inverse $\boldsymbol{J_{FLEXT}}^+$ by the task $\boldsymbol{\Delta x_{FLEXT}}$ gives the expected $\Delta\theta$. Most likely the task $\boldsymbol{\Delta x_{FLEXT}}$ will be scaled down by the linearized IK framework to suit the small variation requirement (section 4) but in any case the solution will be proportional to $\Delta\theta$. The key point to note is that, once the coupled joint variations are expressed in $\boldsymbol{J_{FLEXT}}$, <u>the corresponding one dimensional joint variation subspace cannot be exploited by lower priority constraints</u> owing to the projection operator (equ. (3)).

5.3 Handling Singular Contexts

The description provided in the previous section has to be completed to handle the following singular contexts:

- **<u>Null desired displacement $\boldsymbol{\Delta x}$:</u>** this frequent context is singular as it produces a null $\Delta\theta$ that prevents the normalization of the Jacobian (equ. (9)). It would be a mistake to consider that no constraint exists ; instead there IS a constraint of keeping the same location for the effector. So the solution is not to specify the Jacobian as a null line matrix but instead to evaluate it for a ***small virtual displacement*** $\boldsymbol{\Delta x_V}$. This allows to build a non-null jacobian $\boldsymbol{J_{FLEXT}}$ that expresses and locks the one-dimension joint variation subspace acting on this type of displacement. The task itself $\boldsymbol{\Delta x_{FLEXT}}$ is set to zero to be consistent with $\boldsymbol{\Delta x}$.
- **<u>Limb full extension or full flexion :</u>** two contexts are limit cases for which the desired displacement $\boldsymbol{\Delta x}$ may not be totally achievable. For this reason any desired displacement $\boldsymbol{\Delta x}$ must always be checked against potentially reaching these two limits before applying equations (4) to (7). We must have, respectively for the full extension and the full flexion:

$$\mathbf{L3} + \boldsymbol{\Delta x} < \mathbf{L1} + \mathbf{L2} \qquad (12)$$

$$\mathbf{L3} + \boldsymbol{\Delta x} > |\,\mathbf{L1} - \mathbf{L2}\,| \qquad (13)$$

  In case one of these limits is violated the desired displacement is clamped to the limit value. The case of a resulting null clamped displacement has to be treated according to the virtual displacement method described in the previous point. All other cases can be treated with the standard method (sections 5.1 and 5.2).

The methodology described in these two points eradicates the two problems described in section 3. Flexing can always be computed if it is within the limits as it is solved analytically. If the goal is unreachable, out of the limits, the desired displacement is clamped and possibly null. But owing to the virtual displacement method we can identify the joint variation subspace that produces a flexion-extension and we can lock it to prevent its use by lower priority constraints. This second mechanism prevents the rank decrease syndrome

6 Results

We have first performed comparative tests of the convergence performance for two cases of difficult flexing for linearized IK (Fig. 4 a,b,c,e,f). The error amplitude show a regular and much faster decrease with the FLEXT constraint. Figure 4d shows an example of combining the FLEXT constraint with an orientation constraint of the hand.

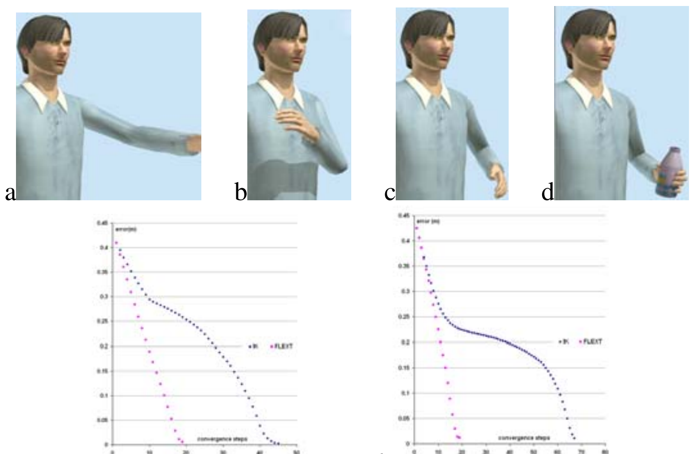

Fig. 4. (a)initial posture, (b) final front flexing, (c) final side flexing (d) final side flexing combined with orientation constraint, (e) front flexing error, (f) side flexing error, IK position constraint (dark diamond), FLEXT constraint (light square)

We have also tested the FLEXT constraint for real-time interactions in which a reduced set of 24 active optical markers were used to track the full body. The critical difference with the previous tests is the nature of the leg control ; although leg and arm have the same limb structure they do not have the same type of task. In a context of "standing reach" the arm effector moves whereas the feet remain static with respect to the floor. Instead the leg root is moving due to the movement of the pelvis and the upper body. Fortunately the integration of the FLEXT constraint into the prioritized IK framework allows to use it transparently for both type of use.

Fig. 5. reduced set of marker used for the real-time full-body interactions

7 Conclusion

Although exploiting a fully analytic approach would allow to solve the postural control in a single computing step, we prefer to comply with the requirement of the small task variation of the linearized IK. Indeed a too large posture variation resulting from the FLEXT constraint would induce a very low validity of the task compensation stage (see [BB04]). Nevertheless the convergence of the overall postural control is improved as shown in the comparative tests. Additional full-body exploitation of this approach will be done in complex environment with obstacles and in conjunction with the use of data-based methods, such as the “motion constraint” introduced in [RB09].

Acknowledgements

This work has been supported by the Swiss National Foundation under the grant N° 200020-117706. Thanks to Mireille for the character design and to Achille Peternier for the MVisio viewer and the CAVE software environment.

References

[NvDR08] Nijholt, A., van Dijk, B., Reidsma, D.: Design of experience and flow in movement-based interaction. In: Egges, A., Kamphuis, A., Overmars, M. (eds.) MIG 2008. LNCS, vol. 5277, pp. 166–175. Springer, Heidelberg (2008)

[LLRE07] Loke, L., Larssen, A.T., Robertson, T., Edwards, J.: Understanding movement for interaction design: frameworks and approaches. Pers. Ubiquit. Comput. 11, 691–701 (2007)

[BMT09] Boulic, R., Maupu, D., Thalmann, D.: On Scaling Strategies for the Full Body Interaction with Virtual Mannequins. Journal Interacting with Computers, Special Issue on Enactive Interfaces 21(1-2), 11–25 (2009)

[BB04] Baerlocher, P., Boulic, R.: An Inverse Kinematic Architecture Enforcing an Arbitrary Number of Strict Priority Levels. The Visual Computer 20(6), 402–417 (2004)

[PMMRTB09] Peinado, M., Meziat, D., Maupu, D., Raunhardt, D., Thalmann, D., Boulic, R.: Full-body Avatar Control with Environment Awareness. IEEE CGA 29(3) (May-June 2009)

[S98] Sturman, D.: Computer Puppetry. IEEE CGA 18(1), 38–45 (1998)

[MGBB07] Michoud, B., Guillou, E., Briceño, H., Bouakaz, S.: Real-Time and Marker-Free 3D Motion Capture for Home Entertainment Oriented Applications. In: Yagi, Y., Kang, S.B., Kweon, I.S., Zha, H. (eds.) ACCV 2007, Part I. LNCS, vol. 4843, pp. 678–687. Springer, Heidelberg (2007)

[A96] Ascension, The Flock of Birds Installation and Operation Guide, Ascension Technology Corporation POB 527 Burlington, Vermont 05402 (802), pp. 860–6440 (1996)

[MBRT99] Molet, T., Boulic, R., Rezzonico, S., Thalmann, D.: An architecture for immersive evaluation of complex human tasks. IEEE TRA 15(3) (1999)

[M*.99] Molet, T., Aubel, A., Capin, T., Carion, S., Lee, E., Magnenat-Thalmann, N., Noser, H., Pandzic, I., Sannier, I., Thalmann, D.: Anyone for tennis? Presence 8(2), 140–156 (1999)

[P], http://www.phasespace.com

[V], `http://www.vicon.com`
[K85] Korein, J.U.: A Geometric Investigation of Reach. MIT Press, Cambridge (1985)
[TGB00] Tolani, D., Goswami, A., Badler, N.I.: Real-Time Inverse Kinematics Techniques for An-thropomorphic Limbs. Graphical Models 62(5), 353–388 (2000)
[KMA05] Kulpa, R., Multon, F., Arnaldi, B.: Morphology-independent Representation of Motions for Interactive Human-like Animation. Computer Graphics Forum 24(3) (2005)
Kallmann, M.: Analytical inverse kinematics with body posture control. Comp. Anim. Virtual Worlds 19(2), 79–91 (2008)
[UPBS08] Unzueta, L., Peinado, M., Boulic, R., Suescun, A.: Full-Body Performance Animation with Sequential Inverse Kinematics. Graphical Models 70(5), 87–104
[BMW87] Badler, N., Manoochehri, K.H., Walters, G.: Articulated figure positioning by multiple constraints. IEEE Comput. Graph. Appl. 7(6), 28–38 (1987)
[PB91] Phillips, C.B., Badler, N.: Interactive behaviors for bipedal articulated figures. Comput. Graph. 25(4), 359–362 (1991)
[ZB94] Zhao, J., Badler, N.: Inverse kinematics positioning using nonlinear programming for highly articulated figures. ACM Trans. Graph. 13(4), 313–336 (1994)
[MBT08] Maupu, D., Boulic, R., Thalmann, D.: Characterizing full-body reach duration across task and viewpoint modalities. On-line Journal of Virtual Reality and Broadcasting 5(15) (November 2008)
[M90] Maciejewski, A.A.: Dealing with the ill-conditioned equations of motion for articulated figures. IEEE CGA 10(3), 63–71 (1990)
Liégeois, A.: Automatic Supervisory Control of the Configuration and Behavior of Multibody Mechanisms. IEEE Transaction on Systems, Man and Cybernetics SMC-7(12), 868–871 (1977)
[SS91] Siciliano, B., Slotine, J.J.: A General Framework for Managing Multiple Tasks in Highly Redundant Robotic Systems. In: Proc. of ICAR 1991, vol. 2, pp. 1211–1215 (1991), ISBN 0-7803-0078-5
[BLP06] Boulic, R., Le Callennec, B., Peinado, M.: Challenges in Exploiting Prioritized Inverse Kinematics for Motion Capture and Postural Control. In: Gibet, S., Courty, N., Kamp, J.-F. (eds.) GW 2005. LNCS (LNAI), vol. 3881, pp. 176–187. Springer, Heidelberg (2006)
[G98] Grassia, F.S.: Practical parameterization of rotations using the exponential map. Journal of graphics tools 3(3), 29–48 (1998); AK Peters
[RB09] Raunhardt, D., Boulic, R.: Motion Constraint. The Visual Computer 25, 509–518 (2009)

Appendix A: General Case

In the general case the human anatomy may deviate from the ideal case used in the prior illustrations of the approach. It may happen that the limb articulated structure does not stand exactly in the flexion-extension plane, for example when the middle flexion axis is not exactly perpendicular to the vector linking the root origin $\mathbf{O_r}$ to the middle joint origin $\mathbf{O_m}$. Another frequent deviation comes from the choice of the controlled effector that may not belong to the FLEXT plane, especially if it corresponds to the location of an optical marker.

Figure 6 illustrates the general definition of the FLEXT plane (i.e. passing through the root origin $\mathbf{O_r}$ with the middle flexion axis as normal) in such a non-ideal case to summarize how the key lengths **L1**, **L2**, **L3** and the offset angle $\boldsymbol{\gamma}$ are computed. The angle γ can be used to detect whether the limb configuration is within the standard limits as illustrated in figure 6 or whether the limb is "overextended", a rare case in which the desired displacement produces a posture variation with opposite sign as the standard case. The overextended case is generally quickly limited by the middle joint limit.

It is important to note that **L1** remains constant as it depends only on the skeleton structure ; in particular it is independent of the twist angle along the first segment linking the limb root to the middle joint because the FLEXT plane rotates together with this twist angle. On the other hand **L2** needs to be updated whenever the twist rotation along the second limb segment changes if the effector is not *on* the twist axis.

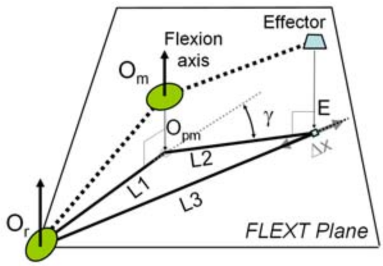

Fig. 6. General case of setting the FLEXT plane and the controlled effector E